Oceanologia (2017) 59, 57—68

Available online at www.sciencedirect.com

ScienceDirect

journal homepage: www.journals.elsevier.com/oceanologia/

ORIGINAL RESEARCH ARTICLE

Testing the performance of empirical remote sensing algorithms in the Baltic Sea waters with modelled and *in situ* reflectance data

Martin Ligi [a,1,*], Tiit Kutser [b,1], Kari Kallio [c], Jenni Attila [c], Sampsa Koponen [c], Birgot Paavel [b], Tuuli Soomets [b], Anu Reinart [a]

[a] *Tartu Observatory, Nõo Parish, Tartu County, Estonia*
[b] *Estonian Marine Institute, University of Tartu, Tallinn, Estonia*
[c] *Finnish Environment Institute, Helsinki, Finland*

Received 4 April 2016; accepted 8 August 2016
Available online 24 August 2016

KEYWORDS
Band-ratio algorithm;
Marine optics;
Baltic Sea

Summary Remote sensing studies published up to now show that the performance of empirical (band-ratio type) algorithms in different parts of the Baltic Sea is highly variable. Best performing algorithms are different in the different regions of the Baltic Sea. Moreover, there is indication that the algorithms have to be seasonal as the optical properties of phytoplankton assemblages dominating in spring and summer are different. We modelled 15,600 reflectance spectra using HydroLight radiative transfer model to test 58 previously published empirical algorithms. 7200 of the spectra were modelled using specific inherent optical properties (SIOPs) of the open parts of the Baltic Sea in summer and 8400 with SIOPs of spring season. Concentration range of chlorophyll-*a*, coloured dissolved organic matter (CDOM) and suspended matter used in the model simulations were based on the actually measured values available in literature. For each optically active constituent we added one concentration below actually measured minimum and one concentration above the actually measured maximum value in order to test the performance of the algorithms in wider range. 77 *in situ* reflectance spectra from rocky (Sweden) and sandy

* Corresponding author at: Tartu Observatory, Observatooriumi 1, Tõravere 61602, Nõo Parish, Tartu County, Estonia. Tel.: +372 51 39 778; fax: +372 696 2555.
E-mail addresses: ligi@to.ee (M. Ligi), tiit.kutser@sea.ee (T. Kutser), kari.y.kallio@ymparisto.fi (K. Kallio), Anu.Reinart@to.ee (A. Reinart).
[1] These authors contributed equally to this work.
Peer review under the responsibility of Institute of Oceanology of the Polish Academy of Sciences.

Production and hosting by Elsevier

http://dx.doi.org/10.1016/j.oceano.2016.08.002

(Estonia, Latvia) coastal areas were used to evaluate the performance of the algorithms also in coastal waters. Seasonal differences in the algorithm performance were confirmed but we found also algorithms that can be used in both spring and summer conditions. The algorithms that use bands available on OLCI, launched in February 2016, are highlighted as this sensor will be available for Baltic Sea monitoring for coming decades.

1. Introduction

Water reflectance data collected with field radiometers has mainly been used for satellite data calibration and validation purposes. However, handheld devices and portable autonomous systems on ferries, jetties, and buoys have become remote sensing tools in their own, as they allow collecting fast and frequent data about the state of waterbodies (Alikas et al., 2015; Groetsch et al., 2014; Simis and Olsson, 2013). Processing the radiometer, as well as satellite data, can be carried out in different ways. A "classical" approach is developing empirical relationships between band-ratios (colour indices), their combinations or more sophisticated parameters and water characteristics, like chlorophyll-*a* concentration. The disadvantages of the empirical methods are that they tend to be local (need tuning for a particular waterbody) or even seasonal (Metsamaa et al., 2006), and need to be developed for each sensor used.

An alternative approach is physics-based analytical methods, where full modelled spectra are used for retrieving chlorophyll-*a*, suspended matter and CDOM (coloured dissolved organic matter) are becoming more and more popular in interpretation of aquatic remote sensing data. Such methods have also been used for more than two decades (Arst and Kutser, 1994; Kutser et al., 2001) and advanced to inversion procedures like Sambuca (Dekker et al., 2011), Bomber (Giardino et al., 2012) retrieving inherent optical water properties (IOPs) and shallow water bottom type simultaneously. There are also neural network type approaches like the method developed for MERIS (Doerffer and Schiller, 2007). The disadvantages of analytical methods, that use water leaving reflectance as the source for water quality parameters calculations, are that they are computationally expensive and require very high-quality input data (*e.g.* perfect atmospheric correction) that is often difficult to achieve. The requirement of high quality input data refers to the spectral library and other model inversion methods. Neural networks can be trained to produce reasonable results even if the reflectance spectra are unrealistic.

It has been shown by many authors (Beltran-Abaunza et al., 2014; Darecki and Stramski, 2004; Kratzer et al., 2008; Reinart and Kutser, 2006) that ocean colour algorithms based on the ratio of blue and green bands (like the OC4v6 developed for retrieving chlorophyll-*a*) provided by different space agencies do not perform well in such optically complex waterbodies like the Baltic Sea. There have been remote sensing activities in different parts of the Baltic Sea and variety of empirical algorithms have been proposed (Attila et al., 2013; Beltran-Abaunza et al., 2014; Darecki et al., 2003, 2005, 2008; Härmä et al., 2001; Koponen et al., 2007; Kowalczuk et al., 2005a, 2010; Kutser, 2004; Kutser et al., 2005a, 2006; Woźniak et al., 2008). However, the algorithms proposed are usually local; applying them in other parts of the sea requires tuning of the algorithms. Moreover, previous studies suggested that there may be need for seasonal water quality algorithms in the Baltic Sea as phytoplankton assemblages in spring and summer are different and their optical properties are very different (Erm et al., 2008; Feistel et al., 2008; Kowalczuk et al., 2005b; Wasmund and Uhlig, 2003). This means that, on the one hand, creating the spectral library necessary for retrieving water properties in the Baltic Sea has to contain reflectance spectra for different seasons. On the other hand, it also suggests that it may be difficult to find band-ratio type algorithms that perform well during the whole year.

As seen in the MERIS ATBD (Doerffer and Schiller, 1997), neural networks have several complicated steps in their calculation. Therefore, the computations may take time, when large satellite images are processed. Empirical algorithms can be used to define initial values for analytical processing to speed up the process by narrowing down the range of variation. For example, the inversion procedures do not have to use the whole spectral library, but only parts of it when approximate concentrations of chlorophyll-*a*, CDOM and suspended matter have been estimated by band-ratio type algorithms. Many satellite instruments are configured to measure water-leaving signal only at a few spectral bands. It means that analytical methods are not always easily usable in interpretation of data from such sensors. Simple band-ratio type remote sensing algorithms are often a good option for retrieving water quality parameters from multispectral data, but these algorithms may also be used in the case of sensors with better spectral resolution as they are computationally fast and easy to use. Therefore, these computationally simple algorithms are also widely used in remote sensing (Ammenberg et al., 2002; Gitelson et al., 2009; Kallio et al., 2001; Koponen et al., 2007).

Our aim was to test whether there are simple empirical algorithms, that use only few spectral channels, which allow estimating chlorophyll-*a*, CDOM and suspended matter concentrations in the Baltic Sea. In an ideal case these algorithms should work all year round, but finding even seasonal algorithms that perform well would be a step forward. The tested algorithms were taken from previously published papers. The reflectance data used in this study was partly simulated with HydroLight radiative model using both summer and spring sets of SIOPs. The concentrations of chlorophyll-*a*, suspended matter and CDOM used in the model simulations covered the whole known range for the Baltic

Table 1 Concentrations used in the spring simulations.

Variable	Concentrations														N
Chl [μg l^{-1}]	0.10	1.0	2.0	4.0	6.0	8.0	10.0	14.0	20.0	26.0	32.0	42.0	84.0	250.0	14
TSM [mg l^{-1}]	0.05	0.4	0.8	1.3	1.8	2.3	4.0	5.7	7.4	8.9	18.0	50.0			12
a_{CDOM}(412) [m^{-1}]	0.05	0.2	0.3	0.5	0.7	0.9	1.2	1.5	3.0	20.0					10

Table 2 Concentrations used in the summer simulations.

Variable	Concentrations												N
Chl [μg l^{-1}]	0.10	0.8	1.7	2.5	3.3	4.2	6.2	8.2	10.2	12.8	26.0	120.0	12
TSM [mg l^{-1}]	0.05	0.2	0.3	0.8	1.3	1.8	3.4	5.0	6.6	8.1	16.0	50.0	12
a_{CDOM}(412) [m^{-1}]	0.05	0.2	0.3	0.5	0.7	0.9	1.2	1.5	3.0	20.0			10

Sea. *In situ* measured data was available for rocky coast of the Baltic Sea (Sweden) and sandy coastal areas (Estonia and Latvia). This datasets allowed evaluating the performance of empirical algorithms for the whole Baltic Sea and two distinctly different seasons. The coastal dataset allowed extending the results to nearshore waters where the concentrations of optically active substances may be beyond those usually observed in the areas reachable by research vessels and were represented by modelled spectra.

2. Material and methods

58 different previously published empirical algorithms were tested. Out of the 58, listed in Table 4, 30 were for chlorophyll-*a* (CHL), 20 for the total suspended matter (TSM) and 8 for coloured dissolved organic matter (CDOM). As some publications give the algorithm with the concentration as the output, but others do not, we have only used the general form of the approaches for comparison (*e.g.* band-ratio to concentration) and calculated the slopes and intercepts from our database. Many algorithms were not used in this study, as they were for case 1 waters and for concentrations too low for the Baltic Sea.

Hydrolight radiative transfer software was used to produce a spectral library of Baltic Sea waters. HydroLight is a commercial software product of Sequoia Scientific, Inc. It is a well-known radiative transfer numerical model that computes radiance distributions and derived quantities, such as irradiances and reflectances, for natural water bodies. Using Hydrolight, spectral radiance distribution can be computed as a function of depth, direction, and wavelength within the water. Water-leaving and reflected-sky radiances are computed separately. HydroLight has to be parameterized with SIOPs of the particular water body under investigation and the number of the optically active substances used in the model can be predefined by the user. The illumination conditions (solar zenith angle, cloudiness) and the state of the sea surface (wind) can be defined by the user. The model uses concentrations of optically active substances as input. A detailed description of the HydroLight software can be found in Mobley and Sundman (2013a, 2013b). Mobley (1994) describes the theoretical basis for the solution of radiative transfer modelling equations. A methodology to use the Hydrolight model for creating spectral libraries in automated Matlab software simulations was generated in the framework of the Finnish national project EOMORE and the EU/FP7 project GLaSS (Global Lakes Sentinel Services). It is shortly described in Attila et al. (2015).

The model simulations were carried out with the SIOPs of summer and spring situations. Concentrations of optically active substances (Tables 1 and 2) were also slightly different. The concentrations were defined based on the statistical distribution of the concentrations in the database collected on R/V Aranda over the Baltic Sea. One concentration below the minimum measured value and one concentration above the measured maximum value were added to the concentration ranges in order to expand the modelling range. The concentrations were selected in the range that should be realistic for the Baltic Sea conditions. The modelled reflectance spectra are shown in Fig. 1.

The main reason of the differences between modelled and measured data is because the modelled spectra are ideal cases, while real measurements include waves, different illumination conditions and other disturbances that occur during real field measurements.

The modelled spectra were simulated using SIOPs of waters sampled from research vessel. Nearshore waters are sometimes optically quite different due to river inflows or resuspension of bottom sediments. In order to expand the open Baltic Sea spectral library (modelled spectra) we used also *in situ* data collected from 77 coastal stations. The data was collected between May and September in Estonia, Latvia and Sweden in 2010—2015 (Figs. 2 and 3, Table 3).

For determination of the concentration of chlorophyll-*a* (in mg m^{-3}), water samples were filtered through Whatman GF/F-filters (0.7 μm pore size) and then extracts of the filters

Table 3 Ranges of measured values.

Variable	Min	Max	Mean
Chl [μg l^{-1}]	0.79	22.38	4.80
TSM [mg l^{-1}]	1.20	18.00	6.26
a_{CDOM}(412) [m^{-1}]	0.28	13.46	2.28

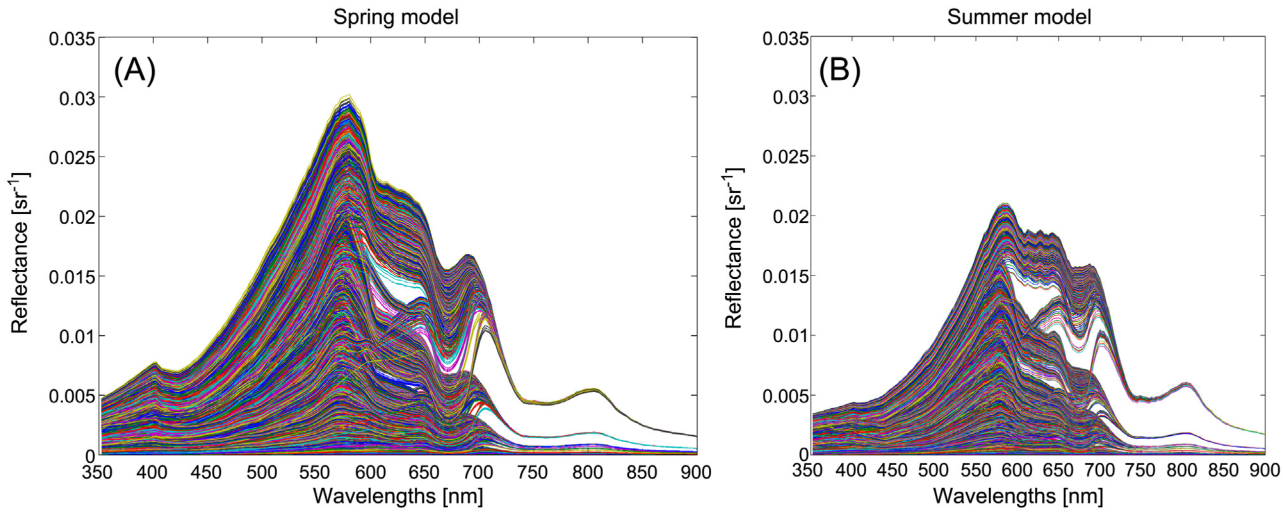

Figure 1 Reflectance (R_{rs}) spectra used in this study: (A) modelled reflectance with spring SIOPs; (B) modelled reflectance with summer SIOPs.

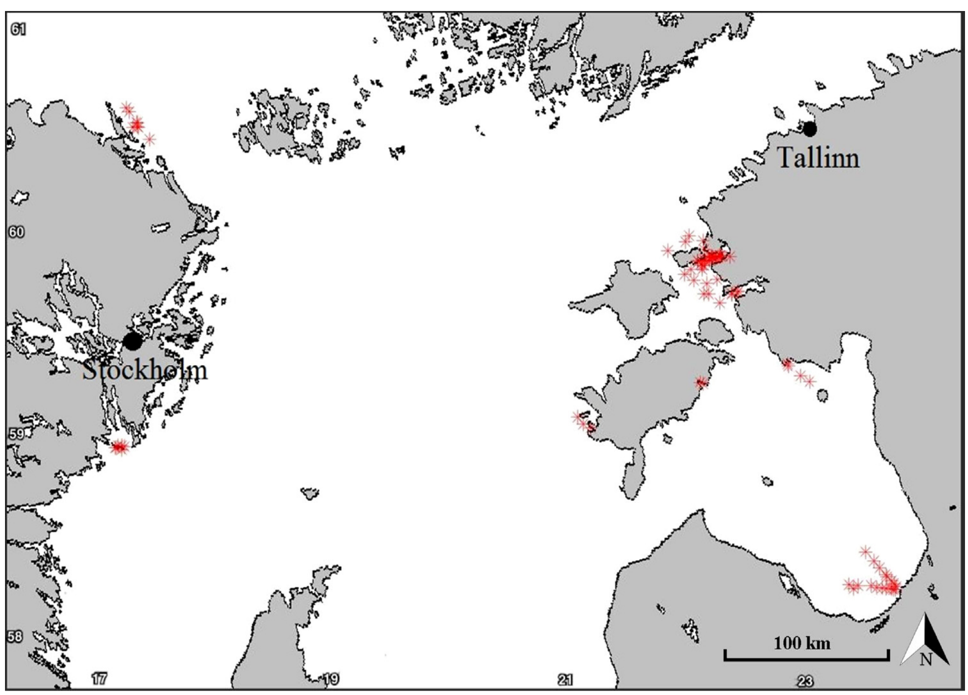

Figure 2 Locations of the sampling points in the coastal waters of the Baltic Sea.

were investigated spectrophotometrically in 96% ethanol according to the ISO standard method (ISO, 1992). Finally, CHL was calculated using the Lorenzen (Lorenzen, 1967) method.

The concentration of total suspended matter (TSM), was measured gravimetrically after filtration of the same amount of water through pre-weighed and pre-combusted (103—105°C for 1 h) GF/F filters. The inorganic fraction of suspended matter, SPIM, was measured after combustion at 550°C for 30 min. The organic fraction of suspended matter, SPOM, was determined by subtraction of SPIM from TSM (ESS, 1993).

Absorption by coloured dissolved organic matter (a_{CDOM}) was measured with a spectrometer (Hitachi U-3010 UV/VIS, at the range of 350—750 nm) in water filtered through a Millipore 0.2 μm filter. Measurements were carried out in a 5-cm cuvette against distilled water and corrected for residual scattering according to Davies-Colley and Vant (1987). $a_{CDOM}(412)$ was used for measuring CDOM concentration in the algorithm analyses. Different algorithms use different wavelengths for CDOM, but as Kowalczuk et al. (2005a) has shown, the slope of the CDOM in the Baltic Sea is relatively stable throughout the year so using a different wavelength as reference should not change the performance of the algorithm.

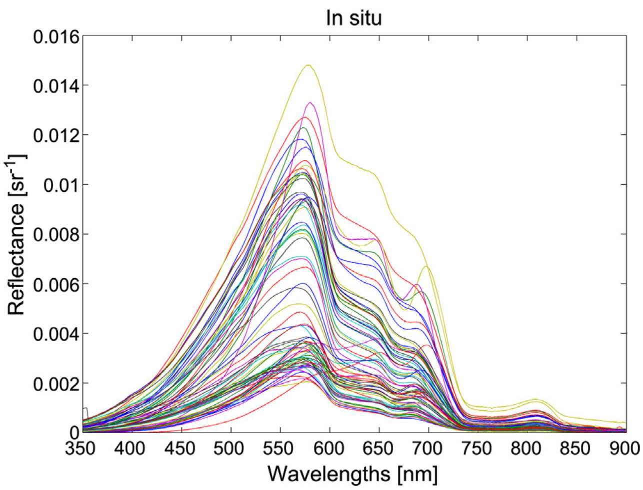

Figure 3 *In situ* measured reflectance (R_{rs}) spectra used in this study.

Above water remote sensing reflectance measurements were carried out with two TriOS RAMSES sensors, where RAMSES-ACC-VIS measures sky irradiance and RAMSES-ARC upwelling radiance. The downwelling irradiance sensor was looking straight up and the upwelling radiance sensor was looking straight down. The methodology was described in more detail in Kutser et al. (2013). RAMSES measures with a 3.3 nm spectral interval at the wavelength range of 350—900 nm. In order to avoid errors in reflectance spectra that occur due to the slight wavelength differences between the two sensors both radiance and irradiance values were interpolated to a 2-nm step before calculating the reflectance as a ratio of upwelling radiance to downwelling irradiance.

To evaluate the performance of the algorithms we used correlation between known concentrations (*in situ* results and model inputs) and algorithm outputs. From the outputs, concentrations were calculated and the mean normalized bias, MNB (systematic error), as well as the normalized rms error (random error), RMS, was calculated, as suggested by Darecki et al. (2005). These errors were defined as follows:

$$\mathrm{MNB} = \mathrm{mean}\left(\frac{x_{calculated} - x_{input}}{x_{input}}\right) \times 100\%,$$

$$\mathrm{RMS} = \mathrm{stdev}\left(\frac{x_{calculated} - x_{input}}{x_{input}}\right) \times 100\%,$$

where $x_{calculated}$ is the chlorophyll concentration estimated from the algorithm and x_{input} is the measured (*in situ*) or model input concentration.

3. Results and discussion

There are no empirical algorithms or other image processing methods that have demonstrated good performance in retrieving chlorophyll-*a*, CDOM or TSM with high accuracy in all parts of the Baltic Sea and during the whole ice-free season. For example the Copernicus Marine Environment Monitoring Service uses chlorophyll-*a* algorithm that has nearly negligible correlation with measured chlorophyll (r^2 = 0.21) (Garnesson and Krasemann, 2016). The latest results by Pitarch et al. (2015) got slightly better results (r^2 = 0.42) with OC4v6. One of the main reasons is optical properties of the Baltic Sea. For example, standard satellite chlorophyll products rely on the ratio of blue and green spectral bands (Darecki and Stramski, 2004). Baltic Sea waters are rich in CDOM that absorbs most of the light in the blue part of the spectrum (Darecki et al., 2003; Kowalczuk et al., 2005b). Therefore, the water leaving radiance in blue is very small. Sun and sky glint also affect the measured signal mostly in the blue part of the spectrum. Consequently, using the blue band in empirical algorithms is not favoured in optically complex waters like the Baltic Sea. Nevertheless, we tested the suitability of a widely used OC4v6 algorithm by means of model simulations. Coefficient of determination between the chlorophyll-*a* concentrations used in the model and estimated based on the simulated reflectance spectra by means of the OC4v6 was poor — R^2 = 0.0054. The results match with the previous findings (Beltran-Abaunza et al., 2014; Darecki and Stramski, 2004; Kratzer et al., 2008; Pitarch et al., 2015; Reinart and Kutser, 2006) that the blue-green ratio is not suitable for retrieval of chlorophyll-*a* in waters where the remote sensing signal in blue part of spectrum is determined by absorption of CDOM not chlorophyll-*a*. On the other hand results by Pitarch et al. (2015) are better than our modelling results. This is surprising as we calculated the OC4v6 from perfect modelled reflectance whereas Pitarch et al. (2015) used satellite data that contains different sources of noise, atmospheric correction errors, *etc*. To certain extent the results by Pitarch et al. (2015) were improved by including about one third of stations from Skagerrak and Kattegat where the physical water properties (salinity) and optical water properties are quite different from the actual Baltic Sea. However, this does not explain all the difference. The results for all other band ratios tested by us are provided in Table 4.

Phytoplankton succession in the Baltic Sea has a strong seasonal component. A spring bloom, dominated by diatoms, starts after ice melts. It is followed by a phytoplankton minimum in June and dominance of cyanobacteria typically in July—August. The optical properties of cyanobacteria differ significantly from other phytoplankton (Groetsch et al., 2014; Kutser et al., 2006; Simis et al., submitted for publication). Therefore, we produced two different spectral libraries — one with SIOPs of spring algal assemblage and one with SIOPs of cyanobacterial season. It was surprising that several band ratio algorithms performed well in estimating CHL, TSM and CDOM from the reflectance spectra of both spring and summer spectral libraries as well as when combined with *in situ* results. It is seen in Figs. 4—7 that the results for spring and summer seasons are slightly different, but some band ratio algorithms provided still acceptable results when spring and summer data was combined. The differences between spring and summer are not large (Fig. 4), but grouping exists and when only results from one season is used, then the statistics are slightly improved. It is also seen in Fig. 4 that the data from most of the *in situ* sampling stations (green circles) fit with the results obtained from modelled spectral libraries. The grouping of points, seen in Fig. 4 (and following figures), occurs because for every chlorophyll concentration used in the model simulation there were several sets with different TSM and CDOM concentrations. This produces the horizontal scattering of points for the same concentration of chlorophyll-*a*. Note that the *in situ* points were not taken into account in calculating the

Table 4 List of algorithms used in this study.

Reference	General form	Code	R^2 IS	MNB% IS	RMS% IS	R^2 model	MNB% model	RMS% model
Chlorophyll								
Zimba and Gitelson (2006)	(1/R650 − 1/R710) × R740	CHL1	0.259	43	99	0.838	305	4581
Moses et al. (2009a)	(1/R665 − 1/R708) × R753	CHL2	0.403	36	93	0.948	−9	1970
Gitelson et al. (2009)	(1/R670 − 1/R710) × R750	CHL3	0.414	35	93	0.964	−144	1750
Mayo et al. (1995)	(R485 − R660)/R570	CHL4	0.194	47	99	0.001	2497	6908
Hunter et al. (2008)	log10(R710/R670)	CHL5	0.499	31	91	0.812	−1021	5477
Han and Jordan (2005)	log10(R482.5)/log10(R660)	CHL6	0.224	45	96	0.003	2475	6880
Schalles et al. (1998)	max(R670 − R850) − (R670 − R850) line value at the location of maximum	CHL7	0.469	41	103	0.041	2270	6456
Brezonik et al. (2005)	R482.5/R660							
	Linear	CHL8	0.172	47	101	0.014	2231	7146
	Exponential		0.219	22	82	0.005	560	1869
	Power		0.191	21	82	0.020	579	1910
Östlund et al. (2001)	R565/(R482.5 + R565 + R660)	CHL9	0.074	55	119	0.020	2333	6887
Wang et al. (2006)	R660/R565	CHL10	0.167	49	104	0.002	2540	7061
Dierberg and Carriker (1994)	R693.5/R679							
	Linear	CHL11	0.556	29	86	0.856	−1125	4198
	Power		0.429	16	75	0.725	119	486
Duan et al. (2007), Menken et al. (2006) and Dierberg and Carriker (1994)	R700/R670	CHL12	0.552	30	88	0.934	−524	2804
Kutser et al. (1999) and Kallio et al. (2001)	R702/R674	CHL13	0.551	30	88	0.951	−522	2569
Koponen et al. (2007) and Ammenberg et al. (2002)	R705/R664	CHL14	0.503	32	94	0.924	−145	2732
Kallio et al. (2003)	R705/R673	CHL15	0.549	30	88	0.957	−399	2337
Kallio et al. (2001)	R706.5/R677.5	CHL16	0.526	31	91	0.966	−447	2317
Kallio et al. (2001) and Moses et al. (2009a)	R707.5/R664	CHL17	0.501	33	93	0.928	−97	2679
Kallio et al. (2001)	R709.5/R673.5	CHL18	0.545	31	88	0.962	−319	2237
Jiao et al. (2006)	R719/R665							
	Linear	CHL19	0.465	35	99	0.938	−48	2736
	Power		0.337	18	82	0.581	226	954
Härmä et al. (2001)	R730/R710	CHL20	0.005	59	121	0.243	1600	6867
Härmä et al. (2001)	R735/R720	CHL21	0.004	58	116	0.127	1956	6507
Moses et al. (2009b)	R748/R667	CHL22	0.163	50	116	0.938	−79	2843
Yacobi et al. (1995)	Rmax(670 − 850)/R670	CHL23	0.397	46	149	0.960	90	869
Schalles et al. (1998)	Sum (R670 − R850) − (sum R670 − R850) Linear	CHL24	0.006	59	119	0.211	1197	7752
Kutser et al. (2016)	R710 − (R676 − R770 linear at R710)	CHL25	0.480	40	97	0.089	1962	5580
Kutser et al. (2016)	R810 − (R770 − R840 linear at R810)	CHL26	0.202	49	111	0.000	2538	7002

Table 4 (*Continued*)

Reference	General form	Code	R^2 IS	MNB% IS	RMS% IS	R^2 model	MNB% model	RMS% model
Anon (2015)	10^(*a* + *b* × *X* + *c* × *X*^2 + *d* × *X*^3 + *e* × *X*^4), *X* = log 10(R489/R555)	CHL27	0.064	55	112	0.005	2504	7004
Darecki et al. (2003)	R550/R590	CHL28	0.160	48	98	0.057	1857	7146
Darecki et al. (2005)	10^(log(*R*(550)/*R*(590)))	CHL29	0.160	48	98	0.057	1857	7146
Woźniak (2014)	R555/R645	CHL30	0.182	47	104	0.049	1998	7141
Total suspended matter								
Dekker et al. (2002)	(R545 + R645)/2							
	Linear	TSM1	0.294	32	80	0.793	−235	690
	Exponential					0.427	142	424
Dekker et al. (2002)	(R565 + R660)/2							
	Linear	TSM2	0.291	32	80	0.794	252	719
	Exponential					0.425	139	418
Kutser et al. (1999)	(Rmax − R750)/(R476 − R750)	TSM3	0.005	45	101	0.000	1899	4437
Kutser et al. (2016)	R810 − (R770 − R840)base	TSM4	0.207	36	86	0.997	86	214
Wang and Ma (2001)	ln((R660 + R825)/(R482.5 + R565))	TSM5	0.014	44	99	0.179	782	3713
Neukermans et al. (2009)	R635/(0.162 − R635)	TSM6	0.260	33	79	0.900	−63	187
Miller and McKee (2004)	R645	TSM7	0.263	33	79	0.913	−139	370
Doxaran et al. (2006) and Wang et al. (2006)	R660/R565							
	Linear	TSM8	0.007	45	100	0.088	1548	3909
	Exponential		0.015	21	83	0.178	433	1330
Kallio et al. (2001)	R702	TSM9	0.230	35	83	0.987	−69	172
Kallio et al. (2001)	R702 − R751	TSM10	0.235	34	81	0.970	−106	266
Koponen et al. (2007) and Ammenberg et al. (2002)	R705	TSM11	0.228	35	83	0.991	−62	152
Thiemann and Kaufmann (2000)	R705/R678	TSM12	0.040	43	98	0.005	1844	4314
Härmä et al. (2001)	R705 − R754	TSM13	0.233	34	81	0.976	−100	249
Kallio et al. (2001)	R709.5	TSM14	0.225	35	84	0.994	−38	91
Doxaran et al. (2003) and Doxaran et al. (2006)	R825/R565							
	Linear	TSM15	0.000	46	102	0.118	1360	3192
	Exponential		0.008	22	86	0.196	367	992
Doxaran et al. (2003) and Onderka and Pekarova (2008)	R840/R545							
	Linear	TSM16	0.000	46	102	0.097	1413	3253
	Exponential		0.003	22	85	0.181	367	972
Doxaran et al. (2002) and Doxaran et al. (2005)	R850/R550							
	Linear	TSM17	0.001	46	101	0.098	1407	3238
	Exponential		0.001	22	85	0.181	367	971
	Polynomial		0.001	42	97	0.181	522	4231
Doxaran et al. (2003)	R855/R55							
	Linear	TSM18	0.001	45	101	0.101	1398	3225
	Exponential					0.183	367	973
Kutser et al. (2016)	R710 − (R676 − R770 linear at R710)	TSM19	0.000	46	102	0.594	932	2207
Woźniak (2014)	R555/R645	TSM20	0.023	44	98	0.163	678	4659

Table 4 (*Continued*)

Reference	General form	Code	R^2 IS	MNB% IS	RMS% IS	R^2 model	MNB% model	RMS% model
Coloured dissolved organic matter								
Brezonik et al. (2005)	R482.5 − 0.657 (R482.5/R825)	CDOM1	0.334	20	99	0.040	720	2019
Koponen et al. (2007)	R663/R490	CDOM2	0.807	21	68	0.827	91	975
Doxaran et al. (2005)	R400/R600							
	Linear		0.337	19	58	0.061	514	2145
	Exponential	CDOM3	0.654	10	50	0.417	127	362
	Power		0.606	10	57	0.631	67	264
Kallio et al. (2008)	R560/R660							
	Linear		0.357	27	67	0.325	144	2615
	Exponential	CDOM4	0.571	14	64	0.636	136	521
	Power		0.464	13	64	0.557	118	535
Kutser et al. (2005a)	R565/R660							
	Linear		0.345	28	70	0.343	133	2603
	Exponential	CDOM5	0.558	15	65	0.636	168	542
	Power		0.448	13	65	0.549	122	560
Ammenberg et al. (2002)	R664/R550	CDOM6	0.791	19	60	0.831	94	1239
Menken et al. (2006)	R670/R571	CDOM7	0.735	22	66	0.796	139	1342
Kowalczuk et al. (2005)	10^(−0.29 − 0.708 × *x* + 1.12 × *x*^2), *X* = log 10(R490/R550)	CDOM8	0.242	24	73	0.000	917	1621

statistics shown in the figure. It is also worth mentioning, that several algorithms were showing very similar results when *in situ* statistics and correlation with modelled data was taken into account, but RMS and MNB values for model data differed significantly. For example the MNB of CHL2 was several times lower than the rest of the algorithms. Also when power function is used, then CHL11 algorithm's MNB and RMS values are relatively low, but correlation is not that good, compared to others.

The results for suspended matter are similar to that of chlorophyll-*a*. The band ratios calculated from *in situ* reflectance spectra are not correlating well with the TSM concentrations. However, if the *in situ* results are plotted together with the results obtained from modelled reflectance spectra

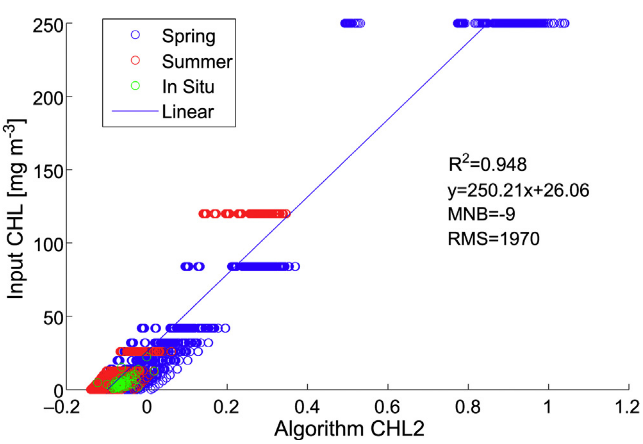

Figure 4 Correlation between the chlorophyll algorithm No. 2 — (1/R665 — 1/R708) × R753 (Moses et al., 2009a) and chlorophyll concentrations [μg l^{-1}] measured *in situ* (for green circles) or used in the model simulations (red — summer and blue — spring circles). Determination coefficients for summer and spring data separately are r^2 = 0.96 and 0.94 respectively. Correlation for the field data separately was lower (r^2 = 0.40).

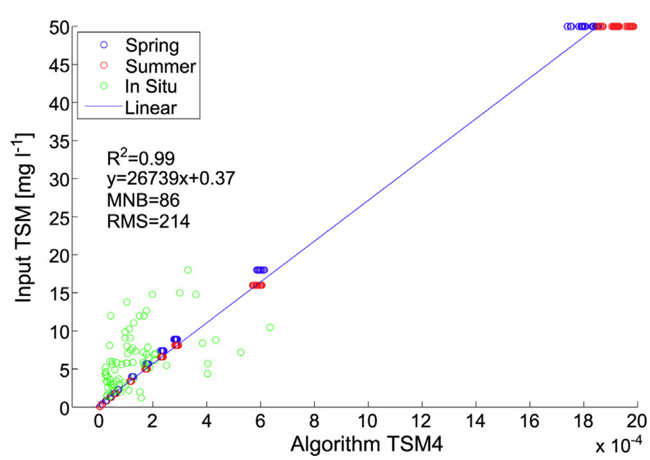

Figure 5 Correlation between TSM algorithm No. 4 — R812 — (R770 — R840)base (Kutser et al., 2016) and the TSM values [mg l^{-1}] used in model simulations (red — summer and blue — spring circles) or measured *in situ* (green circles). Note that the determination coefficient in the figure is for modelling results and does not include *in situ* data. For *in situ* data r^2 = 0.210.

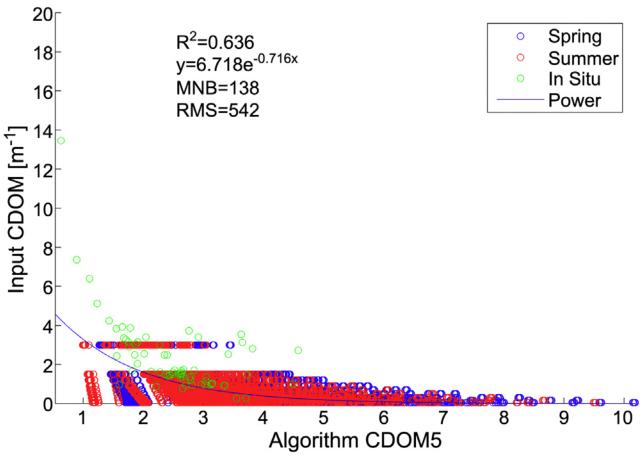

Figure 6 Correlation between CDOM algorithm No. 5 — R565/R660 (Kutser et al., 2005) and the CDOM values [m^{-1}] used in model simulations (red — summer and blue — spring circles) or measured *in situ* (green circles). Note that the determination coefficient in the figure is for modelling results and does not include *in situ* data.

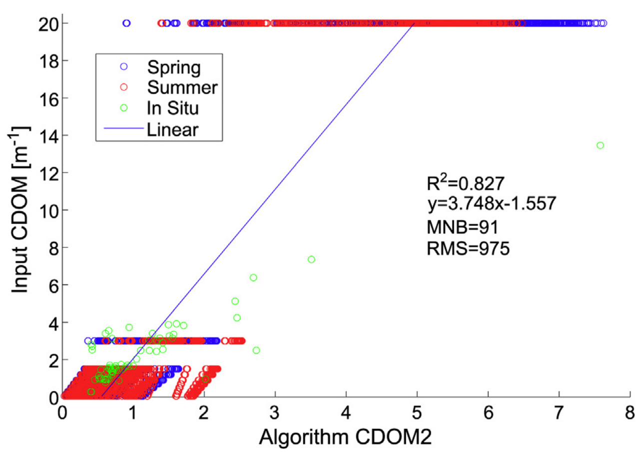

Figure 7 Correlation between CDOM algorithm No. 2 — R663/R490 (Koponen et al., 2007) and the CDOM values [m^{-1}] used in model simulations (red — summer and blue — spring circles) or measured *in situ* (green circles). Note that the determination coefficient in the figure is for modelling results and does not include *in situ* data.

then they fit with the general trend. For example, the correlation between the 810 nm peak height (Kutser et al., 2016) and the TSM concentration was very high (r^2 close to 1) if we used only modelled spectra, but very low for *in situ* data (r^2 = 0.29). On the other hand, *in situ* values follow the trend from the model data (Fig. 5). The higher variation in *in situ* data may be caused by the fact that mineral to organic ratio in suspended matter is highly variable in near coastal waters. The amount of mineral particles may be high due to resuspension in shallow water areas or river inflow but the amount of mineral particles should be minimal in open parts of the Baltic Sea due to sedimentation. On the other hand the modelled spectral library was created using SIOPs of open Baltic Sea waters where the TSM was predominantly phytoplankton. Interesting phenomenon is with algorithms TSM6 and TSM16. Both show good results, but tend to overestimate the tsm concentrations for *in situ* data, compared to underestimation for the model data.

For CDOM we found results that are just the opposite compared to the CHL and TSM example — some algorithms gave better results with *in situ* data than against simulated data. For example, the green circles (*in situ* data) in Fig. 6 follow the power law function between green/red band ratio and CDOM better than the band-ratio calculated from modelled spectra (red and blue circles). One explanation that comes out from Fig. 6 is that CDOM retrieval with this algorithm is problematic if CDOM values are low, but chlorophyll and TSM values vary in great extent. Lower CDOM values usually occur in the middle of the Baltic Sea where TSM is also low and chlorophyll values are high only during bloom situations. This means that this band-ratio algorithm may actually work better than predicted by Fig. 6 modelling part as situations where CDOM is low, but TSM and chlorophyll are high, are not very probable in the Baltic Sea. Such situation may occur either in bloom conditions or in river estuaries bringing low CDOM turbid waters to the Baltic Sea. If all the statistics are taken into account, then the CDOM2 (Koponen et al., 2007, Fig. 7) tends to show the best results.

Most of the successful CHL algorithms used the peak near 700—710 nm. Many algorithms use the ratio of this peak to minima in reflectance caused by chlorophyll-*a* absorption (using bands near 675 nm). Such band combinations are available on both Sentinel 3 OLCI and Sentinel 2 MSI sensors. OLCI data has 300 m spatial resolution that is too coarse in many geomorphologically sophisticated coastal areas of the Baltic Sea. Sentinel 2 will provide similar band configuration (665 nm and 705 nm) with 20 m spatial resolution. We have demonstrated (Toming et al., 2016) that the height of the 705 nm peak in MSI data is very useful for mapping lake chlorophyll, but Sentinel 2 should perform as well in coastal regions with sophisticated geomorphology. It has been demonstrated (Kutser, 2004) that 30 m spatial resolution is not sufficient in the case of cyanobacterial blooms and the chlorophyll concentration may vary by more than two orders of magnitude within one 300 m pixel. Optical water properties may vary as dramatically in river estuaries. Therefore, the launch of Sentinel 2 opened a great new potential in coastal and inland water studies. Sentinel 2 imagery will be available nearly every second day when both S2a and S2b are on orbit, meaning that the high resolution monitoring of coastal waters becomes feasible from technical point of view and there are suitable algorithms for retrieving water quality parameters.

The most successful TSM algorithm used the height of 810 nm peak as a descriptor of suspended matter concentration whereas other good algorithms used the height of the peak at 700—710 nm. Both Sentinel 2 and Sentinel 3 have spectral bands in the 700—710 nm peak region as was mentioned above. We have demonstrated (Kutser et al., 2016) that the Sentinel 2 MSI band 7 (783 nm) can be used to detect the peak at 810 nm although the spectral band is not located optimally to capture this feature. Sentinel 3 OLCI has band 16 at 778.75 nm. It should potentially be used in the same way like the MSI 783 nm band, but this has to be tested with real data.

One of the useful CDOM retrieval algorithms is based on the blue to red band ratio whereas others are based on the red to green band ratio. In general, use of the blue band in retrieving CDOM is hampered by low water leaving radiance in CDOM-rich waters. Another issue is atmospheric correction that has the largest errors in the blue part of spectrum. It has been demonstrated in the case of lakes (Kutser et al., 2005b) that green to red band ratios perform the best in retrieving CDOM content of the water. We have also demonstrated with Sentinel 2 imagery that the band ratio works well in retrieving CDOM concentrations in lakes (Toming et al., 2016). Therefore, one may assume that the band ratio works well also in the CDOM-rich coastal waters of the Baltic Sea.

Most of the spectral bands used in the successful band-ratio algorithms match with the Sentinel 3 OLCI band configuration or are very close to it. This suggests that the empirical algorithms can be used in retrieving concentrations of CHL, TSM and CDOM in the Baltic Sea provided atmospheric correction of the imagery produces reliable reflectance spectra. According to our results, the best OLCI channel ratios to use for chlorophyll retrieval are band11/band9 (CHL14 — chla = $89.97 \times$ R705/R664 $-$ 66.10) and band11/band10 (CHL16 — chla = $82.10 \times$ R706.5/R677.5 $-$ 63.38); as the OLCI sensor bands are wider, these bands also include wavelengths used in this study. As the OLCI sensor does not have a band near 810 nm, band11-band12 (TSM13 tsm = $5670.34 \times$ (R705 $-$ R754) $-$ 0.53 and TSM14 tsm = $4141.74 \times$ R709.5 $-$ 0.23) might be something that is worth testing. OLCI bands match very well with our best CDOM results (CDOM6 — band8/band6 — cdom412 = $10.80 \times$ R664/R550 $-$ 2.82) and CDOM2 (band8/band4 — cdom412 = $3.75 \times$ R663/R490 $-$ 1.56).

4. Conclusions

The results confirm the assumption that seasonal remote sensing algorithms provide the best results in the Baltic Sea. However, the results of the study also show that there are band ratio algorithms that can be used all year round to get reliable estimates of chlorophyll-*a*, CDOM and TSM.

Several of the best performing algorithms use spectral bands available on both Sentinel 2 and Sentinel 3 meaning that these satellites can be used in retrieving concentrations of optically active substances in the Baltic Sea by means of band ratio algorithms. We would recommend using CHL14 (Ammenberg et al., 2002; Koponen et al., 2007) and CHL16 (Kallio et al., 2001) for chlorophyll-*a* retrieval, TSM13 (Härmä et al., 2001) and TSM14 (Kallio et al., 2001) for total suspended matter, and CDOM2 (Koponen et al., 2007) and CDOM6 (Ammenberg et al., 2002) for cdom absorption.

Acknowledgements

Field data used in this study was collected in the framework of the Interreg IVA project Hispares and the PECS project "Simulating Performance of ESA Future Satellites for Water Quality Monitoring of the Baltic Sea". Model simulation and analysis were supported by the Finnish national project EOMORE, the BONUS program project FerryScope, the European Comission programs GLaSS and WaterS; and the Republic of Estonia Ministry of Education and Research grants SF0180009As11 and SF0180009Bs11.

References

Alikas, K., Kango, K., Randoja, R., Philipson, P., Asuküll, E., Pisek, J., Reinart, A., 2015. Satellite-based products for monitoring optically complex inland waters in support of EU Water Framework Directive. Int. J. Remote Sens. 36 (17), 4446—4468, http://dx.doi.org/10.1080/01431161.2015.1083630.

Ammenberg, P., Flink, P., Lindell, T., Pierson, D., Strombeck, N., 2002. Bio-optical modelling combined with remote sensing to assess water quality. Int. J. Remote Sens. 23 (8), 1621—1638, http://dx.doi.org/10.1080/01431160110071860.

Anon, 2015. OCV6 (Ocean Color Chlorophyll (OC) v6), http://oceancolor.gsfc.nasa.gov/cms/reprocessing/r2009/ocv6.

Arst, H., Kutser, T., 1994. Data processing and interpretation of sea radiance factor measurements. Polar Res. 13 (1), 3—12.

Attila, J., Kallio, K., Kutser, T., Koponen, S., Simis, S., Böttcher, M., Brockmann, C., 2015. FerryScope D2.1 Hydrolight Baltic, Version 1.2. 30.06.2015.

Attila, J., Koponen, S., Kallio, K., Lindfors, A., Kaitala, S., Ylöstalo, P., 2013. MERIS Case II water processor comparison on coastal sites of the northern Baltic Sea. Remote Sens. Environ. 128, 138—149, http://dx.doi.org/10.1016/j.rse.2012.07.009.

Beltran-Abaunza, J.M., Kratzer, S., Brockmann, C., 2014. Evaluation of MERIS products from Baltic Sea coastal waters rich in CDOM. Ocean Sci. 10, 377—396, http://dx.doi.org/10.5194/os-10-377-2014.

Brezonik, P., Menken, K.D., Bauer, M., 2005. Landsat-based remote sensing of lake water quality characteristics, including chlorophyll and colored dissolved organic matter (CDOM). Lake Reserv. Manage. 21 (4), 373—382, http://dx.doi.org/10.1080/07438140509354442.

Darecki, M., Ficek, D., Krezel, A., Ostrowska, M., Majchrowski, R., Wozniak, S.B., Bradtke, K., Dera, J., Wozniak, B., 2008. Algorithms for the remote sensing of the Baltic ecosystem (DESAMBEM). Part 2: Empirical validation. Oceanologia 50 (4), 509—538.

Darecki, M., Kaczmarek, S., Olszewski, J., 2005. SeaWiFS ocean colour chlorophyll algorithms for the southern Baltic Sea. Int. J. Remote Sens. 26 (2), 247—260, http://dx.doi.org/10.1080/01431160410001720298.

Darecki, M., Stramski, D., 2004. An evaluation of MODIS and SeaWIFS bio-optical algorithms in the Baltic Sea. Remote Sens. Environ. 89 (3), 326—350, http://dx.doi.org/10.1016/j.rse.2003.10.012.

Darecki, M., Weeks, A., Sagan, S., Kowalczuk, P., Kaczmarek, S., 2003. Optical characteristics of two contrasting Case 2 waters and their influence on remote sensing algorithms. Cont. Shelf Res. 23 (3—4), 237—250, http://dx.doi.org/10.1016/S0278-4343(02)00222-4.

Davies-Colley, R.J., Vant, W.N., 1987. Absorption of light by yellow substance in freshwater lakes. Limnol. Oceanogr. 32 (2), 416—425, http://dx.doi.org/10.4319/lo.1987.32.2.0416.

Dekker, A.G., Phinn, S.R., Anstee, J., Bissett, P., Brando, V.E., Casey, B., Fearns, P., Hedley, J., Klonowski, W., Lee, Z.P., Lynch, M., Lyons, M., Mobley, C., Roelfsema, C., 2011. Intercomparison of shallow water bathymetry, hydro-optics, and benthos mapping techniques in Australian and Caribbean coastal environments. Limnol. Oceanogr. Meth. 9 (9), 396—425, http://dx.doi.org/10.4319/lom.2011.9.396.

Dekker, A.G., Vos, R.J., Peters, S.W., 2002. Analytical algorithms for lake water TSM estimation for retrospective analyses of TM and SPOT sensor data. Int. J. Remote Sens. 23 (1), 15—35, http://dx.doi.org/10.1080/01431160010006917.

Dierberg, F.E., Carriker, N.E., 1994. Field testing two instruments for remotely sensing water quality in the Tennessee Valley. Environ. Sci. Technol. 28 (1), 16—25, http://dx.doi.org/10.1021/es00050a004.

Doerffer, R., Schiller, H., 1997. Algorithm Theoretical Basis Document (ATBD 2.12). Pigment Index, Sediment and Gelbstoff Retrieval from Directional Water Leaving Radiance Reflectances using Inverse Modelling Technique. GKSS Research Centre.

Doerffer, R., Schiller, H., 2007. The MERIS Case 2 algorithm. Int. J. Remote Sens. 28 (3—4), 517—535, http://dx.doi.org/10.1080/01431160600821127.

Doxaran, D., Castaing, P., Lavender, S., 2006. Monitoring the maximum turbidity zone and detecting finescale turbidity features in the Gironde estuary using high spatial resolution satellite sensor (SPOT HRV, Landsat ETM) data. Int. J. Remote Sens. 27 (11), 2303—2321, http://dx.doi.org/10.1080/01431160500396865.

Doxaran, D., Cherukuru, R., Lavender, S., 2005. Use of reflectance band ratios to estimate suspended and dissolved matter concentrations in estuarine waters. Int. J. Remote Sens. 26 (8), 1763—1770, http://dx.doi.org/10.1080/01431160512331314092.

Doxaran, D., Froidefond, J.M., Castaing, P., 2002. A reflectance band ratio used to estimate suspended matter concentrations in sediment-dominated coastal waters. Int. J. Remote Sens. 23 (23), 5079—5085, http://dx.doi.org/10.1080/0143116021000009912.

Doxaran, D., Froidefond, J.M., Castaing, P., 2003. Remote-sensing reflectance of turbid sediment-dominated waters. Reduction of sediment type variations and changing illumination conditions effects by use of reflectance ratios. Appl. Opt. 42 (15), 2623—2634, http://dx.doi.org/10.1364/AO.42.002623.

Duan, H.T., Zhang, Y., Zhang, B., Song, K., Wang, Z., 2007. Assessment of chlorophyll-*a* concentration and trophic state for Lake Chagan using Landsat TM and field spectral data. Environ. Monit. Assess. 129 (1), 295—308, http://dx.doi.org/10.1007/s10661-006-9362-y.

Erm, A., Väli, G., Lips, I., Lips, U., 2008. Optical properties of north-eastern Baltic Sea (Conf. paper). In: IEEE/OES US/EU-Baltic Int. Symp. 27—29 May 2008, Tallinn, EEE, http://dx.doi.org/10.1109/BALTIC.2008.4625547 7 pp.

ESS, 1993. EES Method 340.2: Total suspended solids, mass balance (dried at 103—105°C), volatile suspended solids (ignited at 550°C). Environ. Sci. Section, Madison 189—192.

Feistel, R., Günther, N., Wasmund, N., 2008. State and Evolution of the Baltic Sea, 1952—2005: A Detailed 50-year Survey. John Wiley & Sons, Hoboken, 441—481.

Garnesson, P., Krasemann, H., 2016. Quality Information Document. Ocean Colour. Baltic Chlorophyll Observation Products, CMEMS, http://marine.copernicus.eu/documents/QUID/CMEMS-OC-QUID-009-080-097.pdf.

Giardino, C., Candiani, G., Bresciani, M., Lee, Z., Gagliano, S., Pepe, M., 2012. BOMBER: a tool for estimating water quality and bottom properties from remote sensing images. Comput. Geosci. 45, 313—318, http://dx.doi.org/10.1016/j.cageo.2011.11.022.

Gitelson, A.A., Gurlin, D., Moses, W.J., Barrow, T., 2009. A bio-optical algorithm for the remote estimation of the chlorophyll-*a* concentration in case 2 waters. Environ. Res. Lett. 4 (4), 5 pp. 045003.http://iopscience.iop.org/article/10.1088/1748-9326/4/4/045003/meta.

Groetsch, P.M., Simis, S.G., Eleveld, M.A., Peters, S.W., 2014. Cyanobacterial bloom detection based on coherence between ferry-box observations. J. Marine Syst. 140 (A), 50—58, http://dx.doi.org/10.1016/j.jmarsys.2014.05.015.

Han, L., Jordan, K., 2005. Estimating and mapping chlorophyll *a* concentration in Pensacola Bay, Florida using Landsat ETM data. Int. J. Remote Sens. 26 (23), 5245—5254, http://dx.doi.org/10.1080/01431160500219182.

Hunter, P., Tyler, A.N., Willby, N.J., Gilvear, D.J., 2008. The spatial dynamics of vertical migration by *Microcystis aeruginosa* in a eutrophic shallow lake: a case study using high spatial resolution time-series airborne remote sensing. Limnol. Oceanogr. 53 (6), 2391—2406, http://dx.doi.org/10.4319/lo.2008.53.6.2391.

Härmä, P., Vepsäläinen, J., Hannonen, T., Pyhälahti, T., Kämäri, J., Kallio, K., Eloheimo, K., Koponen, S., 2001. Detection of water quality using simulated satellite data and semi-empirical algorithms in Finland. Sci. Total Environ. 268 (1—3), 107—121, http://dx.doi.org/10.1016/S0048-9697(00)00688-4.

ISO 1.1., 1992. Water Quality — Measurement of Biochemical Parameters — Spectrophotometric Determination of Chlorophyll *a* Concentration.

Jiao, H.B., Zha, Y., Gao, J., Li, Y.M., Wei, Y.C., Huang, J.Z., 2006. Estimation of chlorophyll *a* concentration in Lake Tai, China using in situ hyperspectral data. Int. J. Remote Sens. 27 (19), 4267—4276, http://dx.doi.org/10.1080/01431160600702434.

Kallio, K., Attila, J., Härmä, P., Koponen, S., Pulliainen, J., Hyytiäinen, U.-M., Pyhälahti, T., 2008. Landsat ETM+ images in the estimation of seasonal lake water quality in boreal river basins. Environ. Manage. 42 (3), 511—522, http://dx.doi.org/10.1007/s00267-008-9146-y.

Kallio, K., Koponen, S., Pulliainen, J., 2003. Feasibility of airborne imaging spectrometry for lake monitoring — a case study of spatial chlorophyll *a* distribution in two meso-eutrophic lakes. Int. J. Remote Sens. 24 (19), 3771—3790, http://dx.doi.org/10.1080/0143116021000023899.

Kallio, K., Kutser, T., Hannonen, T., Koponen, S., Pulliainen, J., Vepsäläinen, J., Pyhälahti, T., 2001. Retrieval of water quality from airborne imaging spectrometry of various lake types in different seasons. Sci. Total Environ. 268 (1—3), 59—77, http://dx.doi.org/10.1016/S0048-9697(00)00685-9.

Koponen, S., Attila, J., Pulliainen, J., Kallio, K., Pyhälahti, T., Lindfors, A., Rasmus, K., Hallikainen, M., 2007. A case study of airborne and satellite remote sensing of a spring bloom event in the Gulf of Finland. Cont. Shelf Res. 27 (2), 228—244, http://dx.doi.org/10.1016/j.csr.2006.10.006.

Kowalczuk, P., Darecki, M., Zabloka, M., 2010. Validation of empirical and semi-analytical remote sensing algorithms for estimating absorption by colored dissolved organic matter in the Baltic Sea from SeaWiFS and MODIS imagery. Oceanologia 52 (2), 171—196, http://dx.doi.org/10.5697/oc.52-2.171.

Kowalczuk, P., Olszewski, J., Darecki, M., Kaczmarek, S., 2005a. Empirical relationships between coloured dissolved organic matter (CDOM) absorption and apparent optical properties in Baltic Sea waters. Int. J. Remote Sens. 26 (2), 345—370, http://dx.doi.org/10.1080/01431160410001720270.

Kowalczuk, P., Ston-Egiert, J., Cooper, W.J., Whitehead, R.F., Duranko, M.J., 2005b. Characterization of chromophoric dissolved organic matter (CDOM) in the Baltic Sea by excitation emission matrix fluorescence spectroscopy. Mar. Chem. 96 (3—4), 273—292, http://dx.doi.org/10.1016/j.marchem.2005.03.002.

Kratzer, S., Brockmann, C., Moore, G., 2008. Using MERIS full resolution data to monitor coastal waters — a case study from Himmerfjärden, a fjord-like bay in the northwestern Baltic Sea. Remote Sens. Environ. 112 (5), 2284—2300, http://dx.doi.org/10.1016/j.rse.2007.10.006.

Kutser, T., 2004. Quantitative detection of chlorophyll in cyanobacterial blooms by satellite remote sensing. Limnol. Oceanogr. 49 (6), 2179—2189, http://dx.doi.org/10.4319/lo.2004.49.6.2179.

Kutser, T., Herlevi, A., Kallio, K., Arst, H., 2001. A hyperspectral model for interpretation of passive optical remote sensing data from turbid lakes. Sci. Total Environ. 268 (1—3), 47—58, http://dx.doi.org/10.1016/S0048-9697(00)00682-3.

Kutser, T., Kallio, K., Eloheimo, K., Hannonen, T., Pyhälahti, T., Koponen, S., Pulliainen, J., 1999. Quantitative monitoring of water properties with the airborne imaging spectrometer AISA. Proc. Estonian Acad. Sci. Biol. Ecol. 48 (1), 25—36.

Kutser, T., Metsamaa, L., Strömbeck, N., Vahtmäe, E., 2006. Monitoring cyanobacterial blooms by satellite remote sensing. Estuar. Coastal Shelf Sci. 67 (1—2), 303—312, http://dx.doi.org/10.1016/j.ecss.2005.11.024.

Kutser, T., Paavel, B., Verpoorter, C., Ligi, M., Soomets, T., Toming, K., Casal, G., 2016. Remote sensing of black lakes and using 810 nm reflectance peak for retrieving water quality parameters of optically complex waters. Remote Sens. 8 (6), 497, http://dx.doi.org/10.3390/rs8060497.

Kutser, T., Pierson, D.C., Kallio, K.Y., Reinart, A., Sobek, S., 2005a. Mapping lake CDOM by satellite remote sensing. Remote Sens. Environ. 94 (4), 535—540, http://dx.doi.org/10.1016/j.rse.2004.11.009.

Kutser, T., Pierson, D.C., Tranvik, L., Reinart, A., Sobek, S., Kallio, K., 2005b. Using satellite remote sensing to estimate the colored dissolved organic matter absorption coefficient in lakes. Ecosystems 8 (6), 709—720, http://dx.doi.org/10.1007/s10021-003-0148-6.

Kutser, T., Vahtmäe, E., Paavel, B., Kauer, T., 2013. Removing glint effects from field radiometry data measured in optically complex coastal and inland waters. Remote Sens. Environ. 133, 85—89, http://dx.doi.org/10.1016/j.rse.2013.02.011.

Lorenzen, C.J., 1967. Determination of chlorophyll and phaeopigments; spectrophotometric equations. Limnol. Oceanogr. 12 (2), 343—346.

Mayo, M., Gitelson, A., Yacobi, Y.Z., Ben-Avraham, Z., 1995. Chlorophyll distribution in Lake Kinneret determined from Landsat Thematic Mapper data. Int. J. Remote Sens. 16 (1), 175—182, http://dx.doi.org/10.1080/01431169508954386.

Menken, K.D., Brezonik, P.L., Bauer, M.E., 2006. Influence of chlorophyll and colored dissolved organic matter (CDOM) on lake reflectance spectra: implications for measuring lake properties by remote sensing. Lake Reserv. Manage. 22 (3), 179—190, http://dx.doi.org/10.1080/07438140609353895.

Metsamaa, L., Kutser, T., Strömbeck, N., 2006. Recognising cyanobacterial blooms based on their optical signature: a modelling study. Boreal Environ. Res. 11 (6), 493—506.

Miller, R.L., McKee, B.A., 2004. Using MODIS Terra 250 m imagery to map concentrations of total suspended matter in coastal waters. Remote Sens. Environ. 93 (1—2), 259—266, http://dx.doi.org/10.1016/j.rse.2004.07.012.

Mobley, C.D., 1994. Light and Water: Radiative Transfer in Natural Waters. Academic Press, San Diego, 608 pp.

Mobley, C.D., Sundman, L.K., 2013a. HydroLight 5.2 — EcoLight 5.2 Technical Documentation. Sequoia Scientific. Inc., 115 pp.

Mobley, C.D., Sundman, L.K., 2013b. HydroLight 5.2 — EcoLight 5.2 Users' Guide. Sequoia Scientific. Inc., 109 pp.

Moses, W.J., Gitelson, A.A., Berdnikov, S., Povaznyy, V., 2009a. Satellite estimation of chlorophyll-*a* concentration using the red and NIR bands of MERIS — the Azov Sea case study. IEEE Geosci. Remote Sci. 6 (4), 845—849, http://dx.doi.org/10.1109/LGRS.2009.2026657.

Moses, W.J., Gitelson, A.A., Berdnikov, S., Povaznyy, V., 2009b. Estimation of chlorophyll-*a* concentration in case II waters using MODIS and MERIS data — successes and challenges. Environ. Res. Lett. 4 (4), 045005, http://dx.doi.org/10.1088/1748-9326/4/4/045005.

Neukermans, G., Ruddick, K., Bernard, E., Ramon, D., Nechad, B., Deschamps, P.-Y., 2009. Mapping total suspended matter from geostationary satellites: a feasibility study with SEVIRI in the Southern North Sea. Opt. Express 17 (16), 14029—14052, http://dx.doi.org/10.1364/OE.17.014029.

Onderka, M., Pekarova, P., 2008. Retrieval of suspended particulate matter concentrations in the Danube River from Landsat ETM data. Sci. Total Environ. 397 (1—3), 238—243, http://dx.doi.org/10.1016/j.scitotenv.2008.02.044.

Östlund, C., Flink, P., Srömbeck, N., Pierson, D., Lindell, T., 2001. Mapping of the water quality of Lake Erken, Sweden, from imaging spectrometry and Landsat Thematic Mapper. Sci. Total Environ. 268 (1—3), 139—154, http://dx.doi.org/10.1016/S0048-9697(00)00683-5.

Pitarch, J., Volpe, G., Colella, S., Krasemann, H., Santoleri, R., 2015. Remote sensing of chlorophyll in the Baltic Sea at basin scale from 1997 to 2012 using merged multisensor data. Ocean Sci. 12 (2), 2283—2313, http://dx.doi.org/10.5194/os-12-379-2016.

Reinart, A., Kutser, T., 2006. Comparison of different satellite sensors in detecting cyanobacterial bloom events in the Baltic Sea. Remote Sens. Environ. 102 (1—2), 74—85, http://dx.doi.org/10.1016/j.rse.2006.02.013.

Schalles, J.F., Gitelson, A.A., Yacobi, Y.Z., Kroenke, A.E., 1998. Estimation of chlorophyll *a* from time series measurements of high spectral resolution reflectance in an eutrophic lake. J. Phycol. 34 (2), 383—390.

Simis, S.G., Olsson, J., 2013. Unattended processing of shipborne hyperspectral reflectance measurements. Remote Sens. Environ. 135, 202—212, http://dx.doi.org/10.1016/j.rse.2013.04.001.

Simis, S.G.H., Ylöstalo, P., Kallio, K., Spilling, K., Kutser, T., Optical biogeochemical models of the Baltic Sea in spring and summer. PLOS ONE, submitted for publication.

Thiemann, S., Kaufmann, H., 2000. Determination of chlorophyll content and trophic state of lakes using field spectrometer and IRS-1C satellite data in the Mecklenburg lake district, Germany. Remote Sens. Environ. 73 (2), 227—235, http://dx.doi.org/10.1016/S0034-4257(00)00097-3.

Toming, K., Kutser, T., Laas, A., Sepp, M., Paavel, B., Nõges, T., 2016. First experiences in mapping lake water quality parameters with Sentinel-2 MSI imagery. Remote Sens. 8, 640, 14 pp.

Wang, F., Han, L., Kung, H.T., Van Arsdale, R.B., 2006. Applications of Landsat-5 TM imagery in assessing and mapping water quality in Reelfoot Lake, Tennessee. Int. J. Remote Sens. 27 (23), 5269—5283, http://dx.doi.org/10.1080/01431160500191704.

Wang, X.J., Ma, T., 2001. Application of remote sensing techniques in monitoring and assessing the water quality of Taihu Lake. Bull. Environ. Contam. Toxicol. 67 (6), 863—870, http://dx.doi.org/10.1007/s001280202.

Wasmund, N., Uhlig, S., 2003. Phytoplankton trends in the Baltic Sea. ICES J. Mar. Sci. 60 (2), 177—186, http://dx.doi.org/10.1016/S1054-3139(02)00280-1.

Woźniak, A.B., 2014. Simple statistical formulas for estimating biogeochemical properties of suspended particulate matter in the southern Baltic Sea potentially useful for optical remote sensing applications. Oceanologia 56 (1), 7—39, http://dx.doi.org/10.5697/oc.56-1.007.

Woźniak, B., Krężel, A., Darecki, M., Woźniak, S.B., Majchrowski, R., Ostrowska, M., Kozłowski, L., Ficek, D., Olszewski, J., Dera, J., 2008. Algorithm for the remote sensing of the Baltic ecosystem (DESAMBEM). Part 1: Mathematical apparatus. Oceanologia 50 (4), 451—508.

Yacobi, Y.Z., Gitelson, A., Mayo, M., 1995. Remote sensing of chlorophyll in Lake Kinneret using high spectral-resolution radiometer and Landsat TM: spectral features of reflectance and algorithm development. J. Plankton Res. 17 (11), 2155—2173, http://dx.doi.org/10.1093/plankt/17.11.2155.

Zimba, P.V., Gitelson, A., 2006. Remote estimation of chlorophyll concentration in hypereutrophic aquatic systems: model tuning and accuracy optimization. Aquaculture 256 (1—4), 272—286, http://dx.doi.org/10.1016/j.aquaculture.2006.02.038.